Earth and Planetary Science Letters, 114 (1993) 259–267
Elsevier Science Publishers B.V., Amsterdam

[CH]

Sedimentation and mixing of a turbulent fluid suspension: a laboratory study

Herbert E. Huppert [a], J. Stewart Turner [b] and Mark A. Hallworth [a]

[a] *Institute of Theoretical Geophysics, Department of Applied Mathematics and Theoretical Physics, University of Cambridge, 20 Silver Street, Cambridge CB3 9EW, UK*

[b] *Research School of Earth Sciences, Australian National University, G.P.O. Box 4, Canberra 2601, ACT, Australia*

Received September 10, 1992; revision accepted November 23, 1992

ABSTRACT

In many geological and industrial situations the mixing that occurs across the moving interface between a turbulent fluid layer and a quiescent layer of different density is of fundamental importance. Much of our knowledge of this process has been obtained from laboratory experiments in mixing boxes where the turbulent motions are generated by the vertical oscillation of a horizontal grid located in the interior of the stirred layer. We report here some experiments in which the turbulent layer contains a suspension of small dense particles, with the stirring grid located at the base of the tank in order to simulate the generation of turbulence by stresses acting at the rough bottom over which it traverses. We compare the data with experiments using dense, but particle-free, fluid layers in the same geometry. The results are distinctly different, since the particles responsible for the density difference between the two layers can also migrate through and fall out of the suspension layer as it changes in thickness. We find that the following equilibrium conditions are attained sequentially as the frequency of stirring, and hence the intensity of turbulence, is increased. The particles eventually all precipitate; or only some precipitate while others are held indefinitely in suspension; or all the particles are suspended by the turbulent motions. Both the last two cases produce a stable self-maintained suspension layer separated from the overlying fluid by a sharp density interface. The results cannot be explained simply in terms of particles falling away from an entraining interface: the work done in keeping the particles in suspension must be taken explicitly into account. The relationship between these experiments, and results previously obtained when the interstitial fluid in the lower sediment layer is less dense than the upper layer and can rise across the interface to drive convective motions above, is also discussed briefly. Our results will be applicable to various sediment-laden flows, including crystal-rich magma layers, pyroclastic flows, avalanches, river outflows, turbidites and the deposition of industrial wastes.

1. Introduction

Gravity currents, or density currents, result whenever fluid of one density flows under gravity into fluid of a different density, either as a horizontal intrusion or along a sloping boundary. When the Reynolds number of the current exceeds approximately 500, the flow is generally turbulent and propagates under a balance between inertial and buoyancy forces. In one of the simplest cases of a gravity current, the density difference is due to thermal differences. Examples of such currents include sea-breezes and katabatic winds in the atmosphere and thermal fronts in the oceans and lakes. A significant part of our knowledge of such gravity currents has been obtained from laboratory experiments using fluids with compositional density differences due to a dissolved component, such as salt or sugar. A very readable account of gravity currents from a broad perspective discussing the results of some of these experiments is contained in [1].

Many naturally occuring flows involve fluids in which bulk density differences are created by suspensions containing solid particles; crystals in convecting magma chambers, fine sand and silt in

Correspondence to: H.E. Huppert, Institute of Theoretical Geophysics, Department of Applied Mathematics and Theoretical Physics, University of Cambridge, 20 Silver Street, Cambridge CB3 9EW, UK.

flowing rivers and ash in volcanic eruption columns are just a few examples. In some situations the particles are passive and have little, or no, dynamic influence on the turbulent flow but are merely transported with it. Examples include very fine ash particles distributed in the atmosphere and microscopic planktonic particles in the oceans. At the other extreme, the suspended particles play a fundamental role in determining the resulting motion. Examples here include avalanches, pyroclastic flows and turbidity currents, which are responsible for the formation of submarine canyons on continental slopes and the transport of silt and sand to the deep oceans. There is still a lot to be understood about the influence of particles in all these situations.

One technique that has been extensively used to study turbulent flows, and in particular to study the entrainment of a fluid of one density by the turbulent motions in an adjacent fluid of different density, has been to use a mixing box, with the turbulence generated mechanically by the vertical oscillation of a horizontal grid of solid bars. The technique was initially introduced by Rouse and Dodu [2], and subsequently extensively used and developed by Turner [3] and also reviewed by him [4,5]. For a comprehensive review from a different perspective of the use of mixing boxes to study turbulent flows devoid of particles the reader is referred to Fernando [6].

In almost all previous experiments the grid of bars has been positioned in the interior of the fluid in order to study the effects of turbulent motions generated by processes far from a solid boundary. We wished to investigate the effects on a flowing suspension layer of the turbulent stresses generated at a rough bottom as the suspension flows over it. We hence needed to introduce two important changes to the standard situation. First, we lowered the grid to oscillate just above the bottom of a mixing box of standard size ($25.4 \times 25.4 \times 45$ cm high) so that the turbulence generation took place at the bottom. All the experiments utilized a square grid made up of 1 cm^2 bars spaced 5 cm centre to centre. The grid oscillation had an amplitude of 1.25 cm and a mean height above the base, $\bar{z}$, of 1.9 cm. A sketch of the system is presented in Fig. 1. Second, in the main series of experiments we replaced the heavy salt solution with a suspension

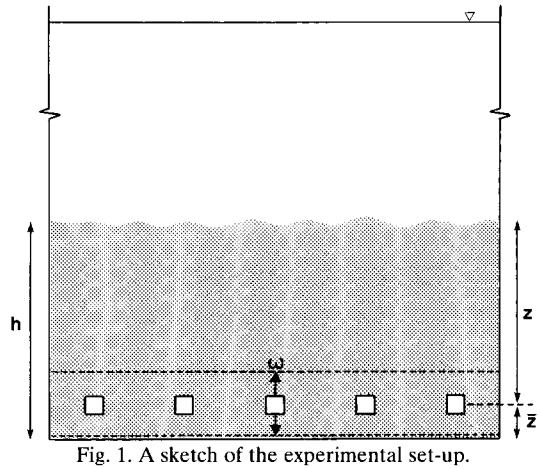

Fig. 1. A sketch of the experimental set-up.

of small silicon carbide particles in water in order to investigate the effect of such particles on the behaviour of the system, especially on the turbulent motions. The overall questions we sought to answer include the following: Is it possible for the turbulent motions to keep the particles indefinitely in suspension? What are the conditions for this? What are the conditions under which only *some* of the particles can be maintained in suspension? And what will be the resulting depth of the suspension layer?

We begin by briefly describing, in the next section, a series of 'calibration' experiments without particles. The experiments quantify the rate at which a turbulent lower layer of relatively dense aqueous sugar solution deepens as it mixes with an overlying less dense fresh water layer due to the oscillation of the grid at the bottom of the tank. In section 3 we then describe the effects due to the bulk density excess in the lower layer being a consequence of a suspension of small particles rather than dissolved sugar. In section 4 we develop a theoretical model which allows us to interpret the laboratory observations and answer the questions posed above. A few further experiments, which help to understand the influence of the boundary conditions imposed at the base of the layer by the oscillating grid, are discussed in section 5. We summarize our results in the final section, which also contains comments on their applications to real situations.

2. Particle-free layers

We first describe briefly the experiments using density differences produced by dissolving sugar in the lower layer. All experiments began with a 6.0 cm layer of sugar solution below a 22 cm layer of pure water. Twenty experiments were carried out with different combinations of grid-oscillation frequencies ω and initial density differences $\Delta\rho_0$. In each case the depth of the lower layer was recorded as a function of time as it deepened due to entrainment of upper layer fluid. Once the depth exceeded 8 cm both the near-grid effects and the difference between the layer depth h and the distance $z(=h-\bar{z})$ between the mean position of the grid and the interface became unimportant, and the observations were well fitted by a power-law relationship of the form

$$z = Bt^b \tag{1}$$

where B is a function of ω and $\Delta\rho_0$ and $b = 0.151 \pm 0.008$. Most previous investigations have used dimensional analysis to express the rate of entrainment at the interface, v_E, in terms of the root-mean-squared horizontal velocity scale just below the interface in the lower layer, v_I, by

$$v_E = \mathrm{d}z/\mathrm{d}t = v_I f(Ri) \tag{2}$$

where f is a function of the Richardson number $Ri = g'h/v_I^2$ and $g' = g\Delta\rho/\rho_0$ is the reduced gravity. Although g' varies with time as the lower layer is diluted, $g'h$, which is approximately $g'z$, is a constant by conservation of solute.

Two separate processes now need to be taken into account, the decay of the turbulent velocity with distance from the grid, and the effect of the resulting v_I on the entrainment across the interface. Further dimensional arguments [5] suggest that

$$v_I = C_1 \omega d^{\alpha+1} z^{-\alpha} \tag{3a}$$

and

$$f(Ri) = C_2 Ri^{-\beta} \tag{3b}$$

for some constants C_1, C_2, α and β, where d is a representative length specified by the geometry of the grid and its stroke [7]. Substituting (3) into (2) and integrating the results, we obtain

$$z = K(g'h)^{-\beta/[\alpha(2\beta+1)+1]}\omega^{(2\beta+1)/[\alpha(2\beta+1)+1]} \times t^{1/[\alpha(2\beta+1)+1]} \tag{4}$$

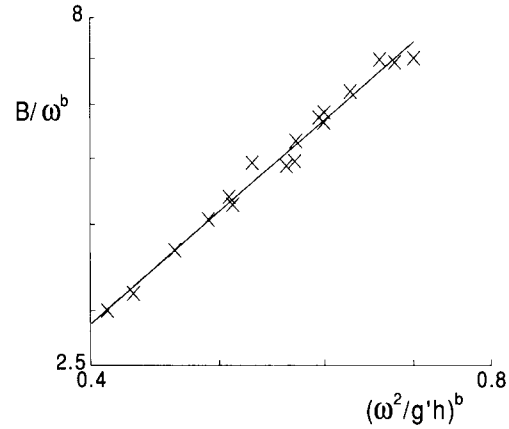

Fig. 2. Experimental data for B/ω^b as a function of $(\omega^2/g'h)^b$ and the line of best fit through the data for experiments with a layer of aqueous sugar solution.

where K is a constant which incorporates the previous constants. Comparing (4) with (1), we see that $\alpha(2\beta+1)+1 = b^{-1} = 6.62 \pm 0.35$ and that another relationship linking α and β can be obtained by comparing the experimentally determined values of B with $K(\omega^2/g'h)^{\beta b}\omega^b$. This is done in Fig. 2, which presents the data for $B\omega^{-b}$ against $(\omega^2/g'h)^b$ on a log-log plot with the best-fit straight line. From the slope of this line we deduce that $\beta = 1.696 \pm 0.072$ and hence that $\alpha = 1.28 \pm 0.11$. These values differ significantly from those previously obtained with the stirring grid located well away from the bottom boundary. A detailed comparison will be deferred for discussion elsewhere. For this paper it suffices to have obtained the results for a grid oscillating near the base in order to compare them with the experiments with a particle-laden layer. This is done in the following sections.

3. Maintenance of a suspension layer

We now present the results of experiments in which the density increase in the lower layer was due to a suspension of silicon carbide grit, which has a density ρ_p of 3.217 g cm^{-3}. Different batches of the irregularly shaped grit particles were used, which have effective diameters ℓ of 5.5, 5.8, 10.8 and 17.6 μm, where the effective diameter is the diameter of a spherical particle with the same low Reynolds number settling velocity. A measured mass M_0 of particles suspended in water was

TABLE 1

Effective grain diameters and critical frequencies

$l(\mu m)$	5.5	5.8	10.8	17.6
$\omega_1\,(s^{-1})$	0.75	0.9	1.0	1.2
$\omega_2\,(s^{-1})$	2.6	2.7	3.4	4.0

added rapidly under a layer of fresh water, before stirring was begun by oscillating the grid with frequency ω. The tank and grid geometry were the same as before. The height of the top of the sediment layer varied in time, but here we will concentrate on the measurements of the final layer properties in the cases where a steady state was attained.

Above a critical frequency ω_2 (see Table 1) dependent only on the size of the particles, all the particles could be held in suspension. For small M_0 the depth of the sediment layer continued to increase up to the free surface, but for sufficiently large M_0 the suspension layer thickness reached a final steady value $h_\infty(=z_\infty+\bar{z})$, which was a function of frequency ω (and also the size of the particles) but independent of the initial thickness of the layer containing the particles. In this regime, where the total mass of particles in suspension is constant, z_∞ is approximately linearly proportional to ω, with the constant of proportionality dependent on the total mass $M_0 \equiv M_\infty$. The final concentration C_∞ of particles in the suspension layer is proportional to M_∞ divided by the final volume of the suspension layer. Below a different critical frequency ω_1 (see Table 1) the intensity of turbulent stirring was insufficient to maintain any of the particles indefinitely in suspension, and eventually they all fell to the floor. The factors determining the equilibrium conditions at the bottom boundary will be discussed further below.

At frequencies between ω_1 and ω_2 some of the particles fell to the floor while a fraction remained suspended in a layer, the final thickness of which was again independent of the initial thickness. The time required to approach the asymptotic state depended on the rate at which mass was lost to the base. During this time the thickness of the suspension layer either changed monotonically or decreased below the equilibrium value and then increased again as mass was gradually lost from the layer, over a time which, in our experiments, was many hours. Quantitative measurements of the final depth of the suspension layer above the grid $z_\infty(=h_\infty-\bar{z})$ as a function of frequency are shown in Figs. 3 and 4a for the whole frequency range covered. (The theory developed below indicates that we should use $z_\infty(z_\infty/h_\infty)^{1/3}$ as the ordinate in these figures, but the difference between z_∞ and h_∞ is so small for most of the data that the plots are changed very little.) These plots include runs with different initial masses and different sizes of particles, and those in which all or only a fraction of the parti-

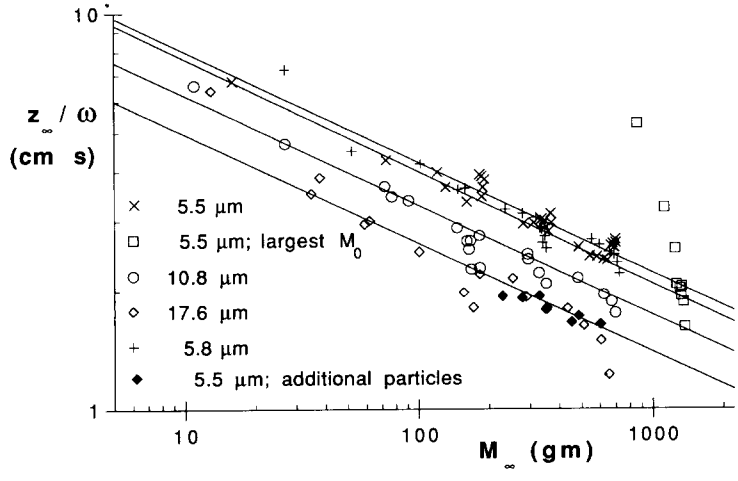

Fig. 3. Experimental data for z_∞/ω as a function of M_∞. Four straight lines of slope -0.275 have been drawn through data obtained from experiments with different sized particles.

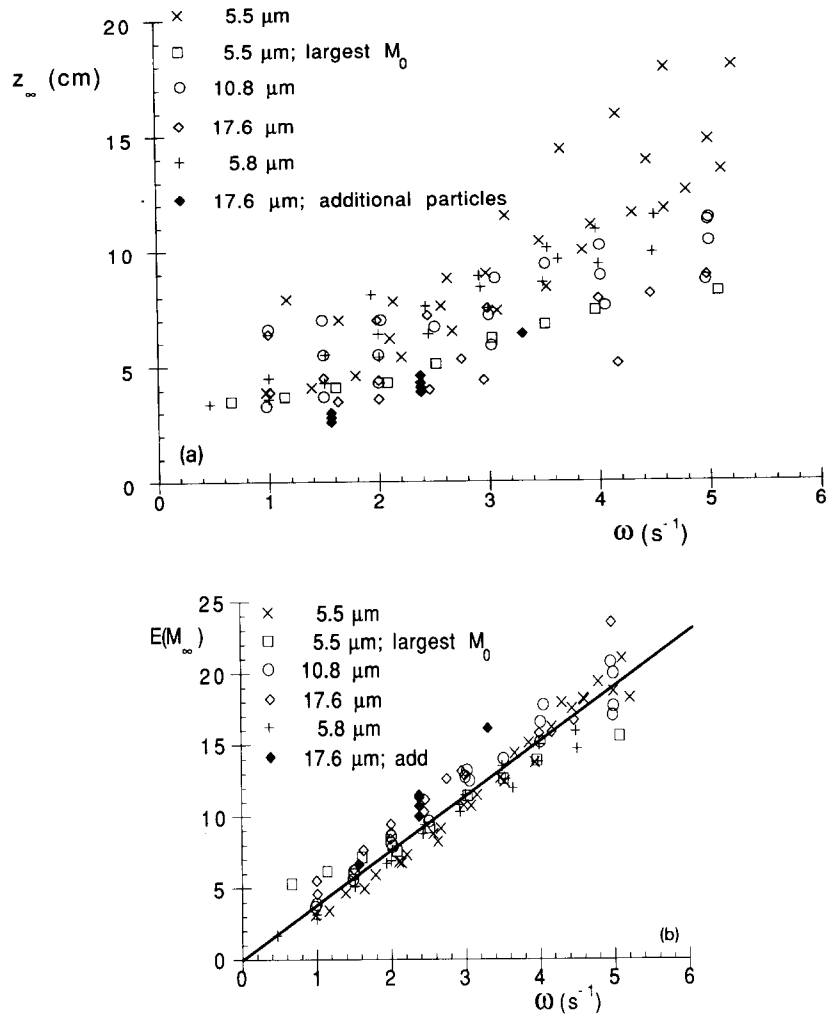

Fig. 4. All the experimental data for (a) z_∞, and (b) the expression $E(M_\infty) = z_\infty(1 + z_o/z_\infty)^{-1/3}(g^* v_s M_\infty / A\rho_p)^{1/3}$ as a function of ω from experiments with different sized particles. The straight line of best fit in (b) has a slope of 3.85.

cles remained in suspension. Figure 3 is a plot of z_∞/ω versus M_∞ for different sized particles on logarithmic scales. In the range $\omega_1 < \omega < \omega_2$ there is good agreement between experiments with a fixed particle size, with the constant of proportionality depending on v_s. When nearly all the particles are in suspension, however, the measured values of z_∞/ω fall below these lines since there is virtually no change in M_∞ (which cannot increase above M_0). Figure 4a plots z_∞ versus ω on linear scales, for comparison with the scaled data on Fig. 4b. In many experiments the size distributions of the sedimented particles and those remaining in suspension were measured and compared. The distributions did not seem to be significantly different, showing that differential settling, with the larger particles falling out first as ω is decreased, is not responsible for the variation of M_∞ with ω.

The linear relationship between z_∞ and ω shown in Fig. 3, with the constant of proportionality being a function of M_∞, suggests that data for a particular mean particle size can be collapsed onto the form $z_\infty M_\infty^\mu \propto \omega$, where the constant of proportionality is a function of the particle diameter ℓ and perhaps some other geometrical factors. The important dynamic effect of variations in particle size is to change the Stokes free

fall speed v_s through the ambient fluid of density ρ_0 (here 1.00 g cm^{-3}) and kinematic viscosity ν through

$$v_s = g(\rho_p - \rho_0)l^2/18\rho_0\nu \tag{5}$$

4. Theoretical explanation

We now consider several alternative theoretical ideas as a guide to the most appropriate method of scaling the data. First, can the eqs. (3) and (4) and the powers α and β, obtained for entrainment across a fluid density interface with exactly the same grid geometry, be carried across to suspensions? The extra hypothesis required is that the sediment layer stops growing when the fall velocity v_s just equals the entrainment velocity v_E. This procedure does not produce a satisfactory collapse of the data, for the following reasons. Differentiating (4) with respect to time in order to determine a relationship for $\mathrm{d}z/\mathrm{d}t = v_E$ and then substituting (4) into the result to determine v_E as a function of z, we find that equating v_s and v_E predicts, with the values of α and β evaluated above, that $z_\infty \propto \omega^{0.78}$. Further if v_E is calculated for all the final layer depths for a given particle size it varies over a wide range, so it cannot be balanced by a fixed settling velocity v_s.

Next we consider theories which include the effect of suspended particles on the dynamics of the whole of a sediment layer. Hopfinger and Linden [8] have shown that when a stabilizing buoyancy flux is added at the boundary of a stirred fluid layer a steady layer depth is attained, with a sharp interface across which the density difference increases linearly in time. Thus the turbulent kinetic energy supplied by the stirring grid is used to increase the potential energy of the system; however, since the turbulent velocity falls to zero at the interface, there can be no question of entrainment. E and Hopfinger [9] extended this idea to layers of sedimenting particles, and Noh and Fernando [10] have proposed a related but considerably more elaborate numerical model. These authors noted that in equilibrium, when the mass of particles in the layer is steady, the upward particle flux due to the turbulent transport must be equal and opposite to the downward flux due to particle settling. Work must be done on the particles to keep them in suspension, and this is equivalent to a stabilizing buoyancy flux which can be related to the settling rate, although because of the two compensating transports, the density of the suspension stays constant and nearly uniform with depth.

The essence of E and Hopfinger's mechanistic theory, which is based on conservation of energy, is contained in the following dimensional argument. The fluid motions near the oscillating grid are described by a single parameter ωd^2, the grid 'action', where d is the representative length scale introduced in (3). The buoyancy flux associated with particles falling out (and being lifted and held in suspension) is $g^* v_s C_\infty$, where C_∞ is the dimensionless volume concentration of particles in the layer and $g^* = g(\rho_p - \rho_0)/\rho_0$ reflects the excess density of the particles relative to that of the fluid, ρ_0. If ωd^2 and $g^* v_s C_\infty$ are the only two physically relevant parameters on which the final depth z_∞ depends, it follows on dimensional grounds that

$$z_\infty = (\omega d^2)^{3/4}(g^* v_s C_\infty)^{-1/4} \tag{6a}$$

Substituting the relationship $M_\infty = A\rho_p h_\infty C_\infty$, where A is the cross-sectional area of the tank, into (6a) and rearranging the terms, we find that

$$z_\infty = (\omega d^2)(g^* v_s M_\infty/A\rho_p)^{-1/3}(1 + \bar{z}/z_\infty)^{1/3} \tag{6b}$$

Rewriting (6b), we find that the function $E(M_\infty)$ defined by

$$E(M_\infty) \equiv z_\infty(1 + \bar{z}/z_\infty)^{-1/3}(g^* v_s M_\infty/A\rho_p)^{1/3} \tag{7a}$$

$$= \omega d^2 \tag{7b}$$

A plot of all the data, scaled using (5) and (7) is shown in Fig. 4b, where different symbols have been used for the four sizes of particles. There is a very satisfactory collapse of the data into a straight line (with the best fit $d = 1.96$ cm), which gives good support to the above theory. The data of E and Hopfinger [9] from experiments with a different grid size and stroke, are well fitted by the same functional form, with a constant $d = 2.7$ cm. We plan to present a more extensive comparison between our model and previous work [9,10] elsewhere.

5. The bottom boundary condition

Our experiments have shown that once the equilibrium sediment load M_∞ in the stirred layer is known, there is good internal consistency between all the measurements of layer depth as a function of ω, v_s and M_∞, and there is theoretical support for the choice of the physically most significant parameters. We still need to consider how M_∞ is related to M_0 when only a fraction of the particles is held in suspension, and, more generally, what determines the 're-entrainment rate' of particles settling on the bottom. To do this the bottom boundary conditions must be examined carefully.

Consider an experiment which started with an initial load M_0, and has reached the stage where some particles have settled on the bottom. Suppose that the particles have been deposited because a given mechanical energy input to the turbulence above the grid can support only a certain (maximum) particle concentration C_∞, and hence maximum buoyancy flux. If ω and hence the energy input are increased, we see from (7) that this general relationship is satisfied if there is an associated increase in M_∞, the mass of particles in suspension, with z_∞ changing little. In fact Fig. 4b contains data for a series of runs for which z_∞ remains approximately constant (within the experimental error) and M_∞ is proportional to ω^3. These results are similar to those obtained by E and Hopfinger [9], and are consistent with their energy argument. They imply that the sediment load is determined mainly by the properties of the turbulence near the grid, and the buoyancy flux through the layer above it.

When M_0 is increased, however, the equilibrium value of z_∞ decreases for a given ω, implying that more particles have been held in suspension because more are available. This behaviour is, we suggest, associated with the fact that the effective turbulent velocity acting on the particles near the bottom is increased when the settled layer of particles is deeper. That is, we now need to consider the detailed geometry of the sediment bed in relation to the grid, and the variation of stirring velocity very close to it, in the space between the mean position of the grid and the floor. In some experiments with the larger values of M_0, the grid, if brought to rest at the bottom of its travel, would be buried in sediment if all the particles settled out. A small extra deposit of sediment would be subjected to a large increase in velocity which would tend to resuspend it.

This interpretation is supported by the results of experiments in which successive charges of sediment were added to the tank while stirring was continued at a fixed frequency (2.38 s^{-1}). For example, starting with 355 g of particles in suspension, a steady state was attained with 230 g of particles left in suspension, and hence 125 g on the floor. Two further additions of 135 g of particles each were made and the suspension layer allowed to come to equilibrium at each stage. Each addition was accompanied by a corresponding decrease in z_∞ but no more particles sedimented during either period. In each case, the values for the final mass in suspension as a function of ω and the other parameters were consistent with (7), as shown by the points marked as a black diamond in Fig. 4b. This result suggests the following interpretation of the lower critical frequency ω_1 shown in Table 1: For each stirring frequency the level of turbulence in the region below the grid allows a critical amount of sediment M_* to settle, and no more, with M_* being a function of ω. At low enough ω, depending on the particle size, all the particles can settle and not be re-entrained. One further result is worth reporting: with the largest values of M_0 used in our experiment, the relationship between z_∞/ω and M_∞ changed dramatically, as shown by the open squares on the right-hand side of Fig. 3. The final depths of the suspension layers were small and the concentrations very high. It seems likely that in this regime the turbulent velocities near the grid were being directly affected by the thickness of the sediment layer on the bottom, and perhaps also by the associated density gradients in the fluid layer.

6. Discussion

Our laboratory experiments and associated theory have yielded an improved understanding of the conditions necessary for the maintenance of a suspension layer and its resulting thickness due to turbulent motions generated by the vertical oscillation of a horizontal grid of square bars. Our theoretical model leads to the relationship

(7), which can be used to predict the thickness of the suspension layer as a function of the oscillation frequency of the grid. The laboratory results are in good agreement with this theoretical prediction. While it is now easy to link conceptually the generation of turbulence at the bottom of a flowing layer of ash or snow particles, crystals or silt with that generated by an oscillating grid, a direct quantitative comparison is unfortunately not yet possible. We can say, however, that heavy particles can be held in suspension by interactions between the flow and the rough bottom it traverses. Further, as the mean flow speed increases the turbulent stresses increase and so does the turbulent intensity. This should be analogous to an increase in ω in the mixing box and hence result in increased values of $E(M_\infty)$.

A theoretical investigation of turbidity currents on a slope has been presented by Parker et al. [11], extending the previous work of these authors [12,13]. The aim of paper [11] was to evaluate possible conditions under which a turbid underflow will pick up a sufficient volume of particles from the bed for the current to maintain its motion down the slope. The analysis involves deriving and solving four nonlinear equations for conservation of fluid, sediment, momentum and turbulent energy, which were related by an entrainment model linking the net amount of sediment taken into the current with the vigour of the turbulent motion within the current. While the approach and aims of Parker et al. are different from ours, it is interesting to note that in both studies the energy required to keep particles in suspension is an important input. Further, our result that below a critical frequency ω_1 no particles can be maintained indefinitely in suspension is mirrored in their 'sediment-entrainment function' E_s, defined in their eq. (22), which is taken from data on suspensions flowing in open channels and is zero for flows whose turbulence level is sufficiently small. Beyond a critical turbulence level E_s increases.

Sparks et al. [14] have carried out laboratory experiments on sediment-laden gravity currents with lighter interstitial fluid flowing initially over a horizontal base. They discussed the application of these currents to brackish underflows in river deltas, turbidity currents and pyroclastic flows. They have examined the processes of sedimentation leading to eventual lift-off in that geometry, but there is still much to be done before the detailed mechanisms are fully understood. With that application in mind too, there will be great experimental advantages in using grid stirring to produce the turbulence in the lower layer, as described in this paper.

We plan also to extend these grid-stirring experiments to explore both the unsteady conditions in which the layer depth is evolving, as well as those cases where the interstitial fluid supporting the particles in the lower layer is less dense than the upper layer fluid. When the latter system is set up with no stirring in the lower layer, the settling of the dense particles leaves behind a thin boundary layer of light interstitial fluid which convects upwards, causing vigorous convective motions in the upper layer and carrying with it some of the sediment. A sharp interface forms, and as Huppert et al. [15] have shown, this descends at a constant velocity which depends on the densities of the layers, the fluid viscosity and explicitly on the size distribution of particles. Note the contrast with experiments using the stirring grid, where only the mean particle size was found to be significant. The lower layer remains stagnant with unimpeded sedimentation, and it is of interest to investigate the effect of mechanical stirring in this layer on the transports across the interface. In particular, is it possible to reach a steady or quasi-steady state when these two competing processes are producing turbulence on opposite sides of the interface? What then determines the thickness of the suspension layer?

Acknowledgements

We are grateful to R.T. Bonnecaze, R.C. Kerr, P.F. Linden, J.R. Lister, H.M. Pantin and E. Wolanski for helpful comments on an earlier version of this work. The experiments were commenced during a visit of JST to Cambridge supported by a grant from the NERC. The research of HEH is supported by the British Petroleum Venture Research Unit.

References

1 J.E. Simpson, Gravity Currents in the Environment and in the Laboratory, Wiley, 1987.

2 H. Rouse and J. Dodu, Turbulent diffusion across a density discontinuity, La Houille Blanche 10, 530–532, 1955.
3 J.S. Turner, The influence of molecular diffusivity on turbulent entrainment across a density interface, J. Fluid Mech. 33, 639–656, 1968.
4 J.S. Turner, Turbulent entrainment: the development of the entrainment assumption and its application to geophysical flows, J. Fluid Mech. 173, 431–471, 1986.
5 J.S. Turner, Buoyancy Effects in Fluids, Cambridge University Press, Cambridge, 1973.
6 H.J.S. Fernando, Turbulent mixing in stratified fluids, Annu. Rev. Fluid Mech. 23, 455–493, 1991.
7 E.J. Hopfinger and J.-A. Toly, Spatially decaying turbulence and its relation to mixing across density interfaces, J. Fluid Mech. 78, 155–175, 1976.
8 E.J. Hopfinger and P.F. Linden, Formation of a thermocline in zero-mean-shear turbulence subject to a stabilizing buoyancy flux, J. Fluid Mech. 114, 157–173, 1982.
9 X. E and E.J. Hopfinger, Stratification by solid particle suspensions, 3rd Int. Symp. Stratified Flows, Caltech, Pasadena, Calif., pp. 1–8, 1987.
10 Y. Noh and H.J.S. Fernando, Dispersion of suspended particles in turbulent flow, Phys. Fluids 3, 1730–1740, 1991.
11 G. Parker, Y. Fukushima and H.M. Pantin, Self-accelerating turbidity currents, J. Fluid Mech. 171, 145–181, 1986.
12 H.M. Pantin, Interaction between velocity and effective density in turbidty flow: phase-plane analysis, with criteria for autosuspension, Mar. Geol. 31, 59–99, 1979.
13 G. Parker, Conditions for the ignition of catastrophically erosive turbidity currents, Mar. Geol. 46, 307–327, 1982.
14 R.S.J. Sparks, R.T. Bonnecaze, H.E. Huppert, J.R. Lister, M.A. Hallworth, H. Mader and J. Phillips, Sediment-laden gravity currents with reversing buoyancy, Earth Planet. Sci. Lett. 114, in press, 1993.
15 H.E. Huppert, R.C. Kerr, J.R. Lister and J.S. Turner, Convection and particle entrainment driven by differential sedimentation, J. Fluid Mech. 226, 349–369, 1991.